

Driven Flows Analysis in a Circular Tube with Non-Newtonian Fluids

Hsiu-Lu Chiang¹, Teng-Lang Feng¹, Jui-Pin Hung²

¹ Department of Mechanical Engineering, Taoyuan Innovation Institute of Technology, No. 414, Sec. 3, Chung Shang E. Road, Chung Li City, Taiwan, R.O.C.

² Department of Mechanical Engineering, National Chin-Yi University of Technology, Taichung 41170, Taiwan

Abstract

A fundamental analysis was conducted to study the internal flow fields of a micropipette system. The flows of the biochemical medicaments are analyzed in the present study by using models of the non-Newtonian fluids to obtain individual responses of the flows from different driven sources. The models of the non-Newtonian fluids adopted for analysing the flows are models of the power-law fluid, the Carreau fluid and the upper-convected Maxwell fluid. Various time-varying pressure gradients and different fluid models are considered in the study. Initial state of the fluid flows in the circular pipette is assumed static, and a start-up time-varying pressure gradient is then applied to the fluid in the pipette. An implicit finite-difference method is used to obtain the numerical approximation solutions of the momentum equation of the flows. The results show the development of the flows in the pipette and the velocity distributions of the non-Newtonian fluids under various pressure gradients, and further obtain the relations between the injected fluid volume and time, providing the flow parameters as a reference for the design of the electrical volume control system that will make the amount of the fluid injected fall accurately within the control margins.

Keywords : Power-law fluid, Carreau fluid, Maxwell fluid, Micropipette system

1. Introduction

In dealing with special, rare and expensive liquids in biochemistry, medicine, medical manufacture and minute chemical engineering, most of the precious liquids have some common characteristics in processing, such as requiring great impulsive force per unit volume, and handling under room temperature and constant volume, etc. The major difficulty of a micro-flow system design and operation is to drive and detect accurately the motions of the fluid. Since the physical quantities are very small and the demand of the accuracy is very high, so choices of a precise driven source and a dynamic control system are the successful keys of the system.

Some of the medicaments, which are on blood base,

produced for the human body in the biochemistry and medicine are not always the Newtonian fluids, but the pseudo-plastic fluids by the categorization of the Rheology, i.e. possessing the properties of shear thinning, from the studies of the Blood Dynamics. If considering the polymer materials, such as blood cells and proteins, the models of the viscoelastic fluids should be used to simulate the flows. Therefore, the flows of the biochemical medicaments are analyzed in the present study by using models of non-Newtonian fluids to obtain individual responses of the flows from different driven sources.

For the temperature sensitive medicaments, the thermal driven may destroy properties of the sample. So, to understand the responses of the isothermal fluid flows driven by a pressure gradient becomes the main subject of the present study. The time periods, signal modal strength and the parameters set-up of the dynamic responses of the electrical control circuits for the driven pressure gradient are all related to the flow rate, flow velocities, friction, properties of the non-Newtonian fluids and the dynamic responses of the flows.

In natural world and industry application, to evaluate the instantaneous characteristics of fluid flow usually causes the complexity of mathematical operations. Since the related dimensions of time-depending flow fields are increased, the analytical and real-time numerical solutions of the momentum and energy equations are difficult to obtain. For the Newtonian fluids, it is easier to solve the numerical solutions in start-up flows. These examples are classical and are commonly placed in textbooks [1-5]. From the viewpoint of biology and considering cases with the elastic and non-elastic tube walls, Etter and Schowalter [6] have solved the flow field of start-up and oscillating pressure gradients in a circular tube for non-Newtonian fluids by using the structural equation of four-term Oldroyd form. The results could predict successfully the influence of some formal stress under a constant shear rate, but can't apply for the case of shear strain.

Okeson and Emery [7] also used the Oldroyd model to solve the problem of moving plate under impact (start-up Couette flow-Stokes' first problem) [8], and showed that, since part of the energy of the flow is stored in the elastic term of the fluid and the rest is used to accelerate the fluid, the time needed to reach the steady state increased obviously. The Rivlin-Ericksen

structural equation was used by Bhatangar [9] to deal with the *i*th instantaneous non-Newtonian fluid field of a fluctuating flow in a porous channel. An oscillating pressure gradient is overlaid to a pressure gradient with fixed values; the fluid was injected to the plane and absorbed to another plane with same amount in the meantime. The phase lags between the velocity and pressure fields were analyzed.

Ly and Bellet [10] developed a model called 'multi-viscosity' approximation method to deal with the instantaneous behaviors of viscoelastic fluids. The procedure is to break the flow field into *N* fixed Newtonian viscosity regions, which can be obtained from the drawn near the non-Newtonian shear stress/shear rate curve. The momentum equation was expressed as the form of shear stress, and then solving different sub-layers to analyze the flow field of circular tube under the oscillating pressure gradient. The laminar flow of an inelastic power-law fluid in a circular tube subjected to both start-up and oscillating pressure gradient condition was studied by Balmer and Fiorina [11]. It was found that the time to reach steady state increased as the power-law index increased and no overshoot phenomena were observed in the flow field. Pontrelli [12] perceived the case of the pulsatile blood flow in a pipe. The unsteady flow of blood in a long pipe, driven by a pulsatile pressure gradient is studied. The results show that, in viscoelastic cases, the shear stress has a phase lead over that in the inelastic cases, but its magnitude stays under theoretic value for all time.

In most cases, we can use simplest and realistic Rheological models to simulate and analyze flow fields. Furthermore, many fluids used in industry and most process, the shear rates of fluids are all within this scope. The purpose of the present study is to solve the momentum equation of the flow in the circular tube by using the viscoelastic model of the non-Newtonian fluids, models adopted are the power-law fluid, the Carreau fluid and the upper-convected Maxwell fluids. Initial state of the flow is assumed static, and a start-up time-varying pressure gradient is then applied to the fluid in the tube. The implicit finite difference method (FDM) is used to obtain the numerical results, and the results are shown and compared with the relational papers.

2. Theory and Analysis

The schematic diagram of the geometry model used for the present study is shown in Fig. 1. The radius and length of the pipette are denoted as *R* and *L* respectively, while the axial direction is represented as *z*. The fundamental assumptions are:

1. Axisymmetric incompressible flow;
2. The circular pipette is located horizontally and the gravity terms can be neglected;
3. The flow is fully-developed and the inertia term

can be neglected;

4. Comparing to the length of the pipette, the radius is relatively small.
5. Along the stream line, the Neumann flow condition is zero ($\partial/\partial\theta=0$).
6. The no-slip condition is used on the solid surface;
7. The driven force is applied along the axial direction.

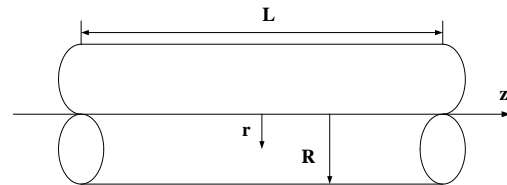


Fig.1 Schematic diagram of flow geometry

The continuity and momentum equations (*z*-direction) in cylindrical form of the flow system are:

$$\frac{1}{r} \frac{\partial}{\partial r}(ru_r) + \frac{1}{r} \frac{\partial}{\partial \theta}(u_\theta) + \frac{\partial}{\partial z}(u_z) = 0 \quad (1)$$

$$\rho \left[\frac{\partial u_z}{\partial t} + (u \cdot \nabla) u_z \right] = -\frac{\partial p}{\partial z} + \rho g_z + \left[\frac{1}{r} \frac{\partial}{\partial r}(rS_{rz}) + \frac{1}{r} \frac{\partial}{\partial \theta}(S_{\theta z}) + \frac{\partial}{\partial z}(S_{zz}) \right] \quad (2)$$

where S_{ij} is the stress tensor. Owing to the assumptions 4 and 5, and the applied pressure gradient is time depending only, from (1), one may obtain the velocity relationship as following:

$$\begin{cases} u_r = 0 \\ u_\theta = 0 \\ u_z = u_z(r, t) \end{cases} \quad (3)$$

If a pressure gradient, $-\partial p/\partial z = f(t)$, is assumed, then, the momentum equation (2) can be expressed as:

$$\rho \frac{\partial u_z}{\partial t} = f(t) + \frac{1}{r} \frac{\partial}{\partial r}(rS_{rz}) \quad (4)$$

1.1 Power-law fluid

Most of the rheology problems of non-Newtonian liquids are due to the comparison of linear domain between $\log \mu$ and $\log \dot{\gamma}$ [13] in the plot. The property of the inclined straight line between shear rate and shear stress in power-law model can be described as:

$$S_{rz} = K \left(\frac{\partial u_z}{\partial r} \right)^n \quad (5)$$

The dimension of K is $pa \cdot s^n$ and n is a dimensionless factor. These parameters are related to the properties of materials and commonly change with the variation of pressure and temperature. Define the following dimensionless parameters:

$$\eta = \frac{r}{R}, \quad \tau = \frac{t}{T}, \quad \phi = \frac{u_z}{W} \quad (6)$$

where $W = (\frac{n}{n+1})(\frac{1}{2K} \frac{\Delta p}{L} R^{n+1})^{1/n}$, $T = \frac{\rho_0 R^{n+1}}{KW^{n-1}}$

Substituting equations (5) and (6) into (4), one may obtain

$$\frac{\partial \phi}{\partial \tau} = 2(\frac{n+1}{n})^n (f(\tau T) \frac{L}{\Delta p}) + \frac{1}{\eta} \frac{\partial}{\partial \eta} (\eta (\frac{\partial \phi}{\partial \eta})^n) \quad (7)$$

If a time depending and periodic pressure gradient is adding to the original fixed pressure gradient, i.e., $f(t) = \Delta p/L + \rho \alpha \sin \omega t$, where ω is the periods, then, equation (8) can be expressed as:

$$\frac{\partial \phi}{\partial \tau} = 2(\frac{n+1}{n})^n (1 + \alpha \sin \beta \tau) + \frac{1}{\eta} \frac{\partial}{\partial \eta} (\eta (\frac{\partial \phi}{\partial \eta})^n) \quad (8)$$

where $\alpha = \rho \alpha L / \Delta p$ and $\beta = \omega T$

1.2 Carreau fluid model

The relationship between shear rate and apparent viscosity of the Carreau fluid model is:

$$\mu_{app} = \mu_{\infty} + (\mu_0 - \mu_{\infty}) [1 + (\lambda_c \dot{\gamma})^2]^{-\frac{n-1}{2}} \quad (9)$$

Where μ_0 and μ_{∞} represent the viscosities at zero shear rate and infinite shear rate respectively, λ_c the relaxation time and $\dot{\gamma}$ the shear rate. Similarly, for the convenience of numerical computation, the following dimensionless parameters are introduced,

$$\eta = \frac{r}{D}, \tau = \frac{tW}{D}, \phi = \frac{u_z}{W}, \mu_0^* = \frac{\mu_0}{\mu_0}, \mu_{\infty}^* = \frac{\mu_{\infty}}{\mu_0}, p^* = \frac{p}{\mu_0 W / D}, z^* = \frac{z}{D} \quad (10)$$

In this model, since the flow pattern is assumed to be creeping flow, so, the reference in dimensionless manipulation for pressure gradient is replaced by the viscous term. Substituting equations (9) and (10) into (4), one have

$$Re_0 \frac{\partial \phi}{\partial \tau} = F(\tau) + \frac{1}{\eta} \frac{\partial}{\partial \eta} \{ \eta [\mu_{\infty}^* + (\mu_0^* - \mu_{\infty}^*) (1 + De^2 (\frac{\partial \phi}{\partial \eta})^2)^{-\frac{n-1}{2}}] \frac{\partial \phi}{\partial \eta} \} \quad (11)$$

where $Re_0 = \rho_0 W D / \mu_0$, $F(\tau) = -\partial p^* / \partial z^*$ and $De = \lambda_c / (D/W)$. The Reynolds number Re represents the ratio of the inertia force to the viscous force, while the Deborah number De [11] is the ratio of the elastic force to the viscous force.

1.3 Upper-convected Maxwell fluid model

The commonly used rheological equation of the upper-convected Maxwell fluid model is in the form of [14],

$$S_{ij} + \lambda \overset{\nabla}{S}_{ij} = 2\mu \dot{\gamma} \quad (12)$$

where λ and μ are the relaxation time and the viscosity respectively, while the symbol ' $\overset{\nabla}$ ' represents the upper-convected derivative. Since the velocity profile is assumed as $u_z = (0, 0, u_z(r, t))$, the unsteady axisymmetric flow, from equations (12) and (4), one

may obtain,

$$S_{rz} + \lambda \frac{\partial S_{rz}}{\partial t} = \mu \frac{\partial u_z}{\partial r} \quad (13)$$

$$\frac{\partial p}{\partial z} = \frac{\partial S_{rz}}{\partial r} + \frac{1}{r} S_{rz} - \rho_0 \frac{\partial u_z}{\partial t} \quad (14)$$

The driven force is applied along the axial direction, and this provides that

$$\frac{\partial p}{\partial r} = \frac{\partial p}{\partial \theta} = 0 \quad (15)$$

Also, from equation (15), one may have $p = p(z, t)$.

By assuming $\partial p / \partial z = -f(t)$, one can eliminate S_{rz} from equation (13) and (14) and obtain,

$$\lambda \frac{\partial^2 u_z}{\partial t^2} + \frac{\partial u_z}{\partial t} - \frac{\mu}{\rho_0} (\frac{\partial^2 u_z}{\partial r^2} + \frac{1}{r} \frac{\partial u_z}{\partial r}) = \frac{1}{\rho_0} (f(t) + \lambda f'(t)) \quad (16)$$

In order to obtain the dimensionless form of momentum equation for subsequent numerical computation, the following dimensionless parameters are defined:

$$\eta = \frac{r}{R}, \tau = \frac{\mu t}{\rho_0 R^2}, \phi = \frac{\mu u_z}{(\Delta p / L) R^2} \quad (17)$$

Substituting (17) into equation (16), one has,

$$H \frac{\partial^2 \phi}{\partial \tau^2} + \frac{\partial \phi}{\partial \tau} - [\frac{\partial^2 \phi}{\partial \eta^2} + \frac{1}{\eta} \frac{\partial \phi}{\partial \eta}] = F(\tau) \quad (18)$$

where $H = \frac{\lambda \mu}{\rho_0 R^2} = \frac{De}{Re}$ and $F(\tau) = -\frac{L}{\Delta p} \frac{\partial p}{\partial z} - H \frac{\partial}{\partial \tau} (\frac{L}{\Delta p} \frac{\partial p}{\partial z})$

1.4 Initial condition

The fluid in the micro-tube is first at rest and then, subjected by the applied pressure gradient to flow, so, the initial condition is,

$$u_z(r, 0) = 0 \quad (19)$$

Or, in the dimensionless form, is

$$\phi(\eta, 0) = 0 \quad (20)$$

1.5 Boundary condition

(1) At wall of the tube ($r=R$), the non-slip condition is

$$u_z(R, t) = 0$$

Or, in the dimensionless form, is

$$\phi(1, \tau) = 0 \quad (21)$$

(2) At center of the tube ($r=0$), the differential boundary condition is

$$\frac{\partial u_z}{\partial r} = 0 \quad (\text{at } r = 0)$$

Or, in the dimensionless form, is

$$\frac{\partial \phi}{\partial \eta} = 0 \quad (\text{at } \eta = 0) \quad (22)$$

3. Numerical method

A simple implicit finite difference method is adopted in this paper. Owing to the non-linearity of the governing differential equation, the linearization must be pre-processed during the numerical iterations. At each time interval, the space iterations must reach a pre-set convergence criteria for the computation to carry on to the next time interval iteration. The convergence criteria of the iteration are:

$$\left| \frac{(\phi_i^k)^{l+1} - (\phi_i^k)^l}{(\phi_i^k)^l} \right| \leq 1 \times 10^{-5} \quad (23)$$

While the convergence criteria for the flow field reaches to steady state is

$$\left| \frac{\phi_i^{k+1} - \phi_i^k}{\phi_i^k} \right| \leq 1 \times 10^{-5} \quad (24)$$

Where l , k and i is the number of iterations, the time index and the space index, respectively.

Using the simple implicit method [15] to solve the approximate solution of the momentum equation, the forward difference scheme is used in time domain, while the space terms are expanded by central difference technique. The computational flow chart is shown in Fig. 2.

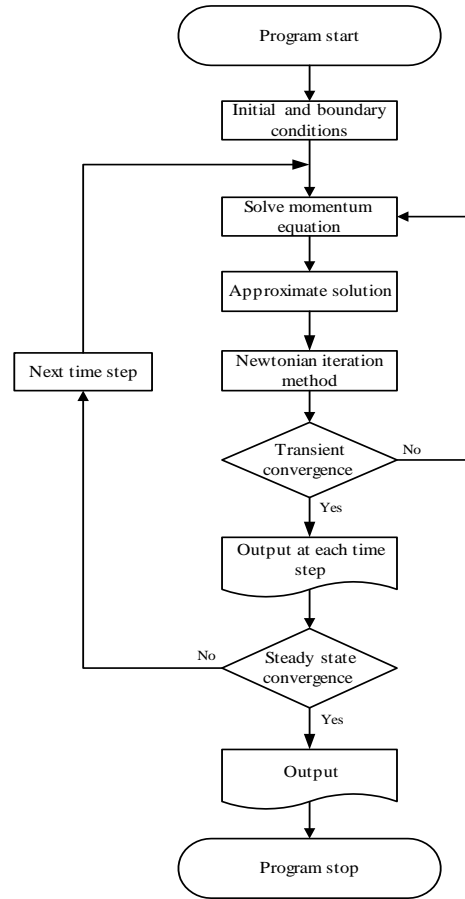


Fig.2 Computational flow chart

4. Results and discussions

4.1 Power-law fluid model

To verify the computational scheme, the numerical results obtained in the present study, with $n=1$ and $f = \Delta p/L$ in equation (7), are compared with the analytic solution obtained by Szymanski and the numerical velocity profiles obtained by Balmer and Fiorina. The comparison has shown a good agreement.

As shown in Fig. 3, if a constant start-up pressure gradient accompanied a sinusoidal variation is applied to the system, for the case with parameters $\alpha=1.0$ and $\beta=2.5$ in equation (8), the results also indicate that the bigger the power-law index n , the faster the flow field reaches the steady state. The results obtained are closely matched to that of Warsi [16].

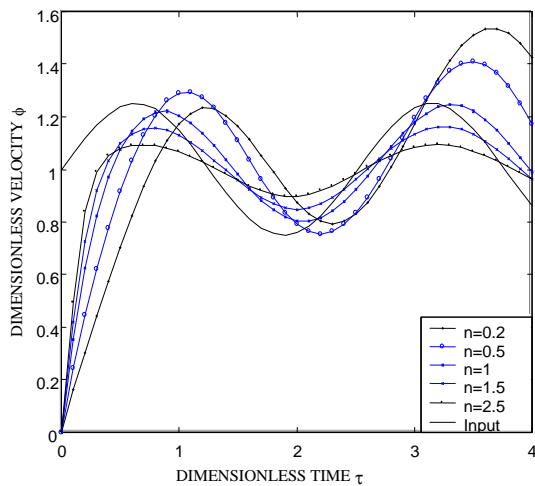


Fig.3 Central velocity vs. time for a constant offset sinusoidal pressure gradient

4.2 Carreau fluid model:

To calculate the momentum equation of Carreau fluid model numerically, the Deborah number De , Reynolds number Re and power-law index n must be determined first. The blood is chosen as the test fluid in this simulation, and the following data are assumed for the blood model as the reference input,

- $\rho_0 = 1.05 \times 10^3 \text{ (kg/m}^3\text{)}$
- $\lambda_c = 3.3135$
- $n = 0.3568$
- $\mu_0 = 56 \text{ (cp)}$
- $\mu_\infty = 3.45 \text{ (cp)}$
- $\dot{m} = 10 \sim 1000 \text{ (}\mu\text{g)}$
- $R = 10 \sim 1000 \text{ (}\mu\text{m)}$

With the cases of mass flow rate $\dot{m} = 100 \mu\text{g/s}$ and radius $R = 100 \mu\text{m}$, the central velocities vs. the dimensionless time τ are shown in Fig. 4. It is obvious that the output velocity is proportional to the input pressure gradient and, at the same amount of mass flow rate, the smaller the pipe radius the larger the central velocity.

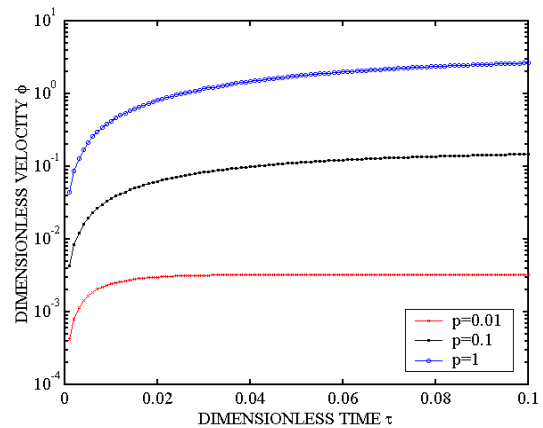


Fig.4 Central velocity vs. time for $\dot{m} = 100 \mu\text{g/s}$ and radius $R = 100 \mu\text{m}$

4.3 Upper-convected Maxwell fluid model:

A constant pressure gradient is applied to the upper-convected Maxwell fluid model for analysis. The variation of the velocity across the pipe at $H = 0.2$, $\tau = 0.1$ is illustrated in Fig. 5. The results are quite well coincident with that of Rahaman and Ramkissoon [14]

It is worth noting to take a comparison of the effect of the viscoelastic term with that of the inertia term, and this can be depicted in parameter H (De/Re). It is clearly; shown in Fig. 6, that the ‘over-shooting phenomenon’ occurs as provided that the viscoelastic effect existing in the fluid model; and the larger the value of H , the larger the amplitude of the over-shooting. On the other hand, it needs more time of the system to reach the steady state as the value of H increases. This can be explained as that, owing to the non-Newtonian fluid possess the viscoelastic characteristic; the system requires more energy to overcome the shear stress due to the flowing of the fluid particles.

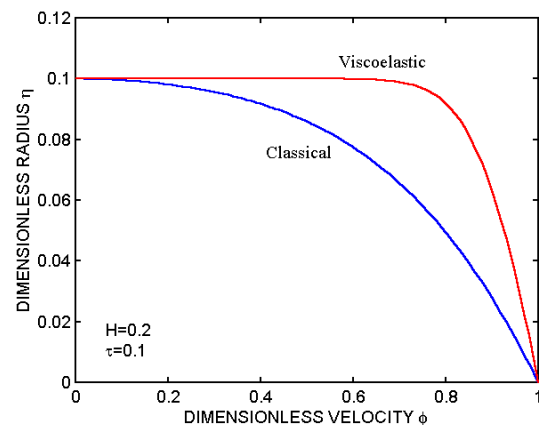


Fig.5 Velocity profiles for a constant pressure gradient ($H = 0.2$; $\tau = 0.1$)

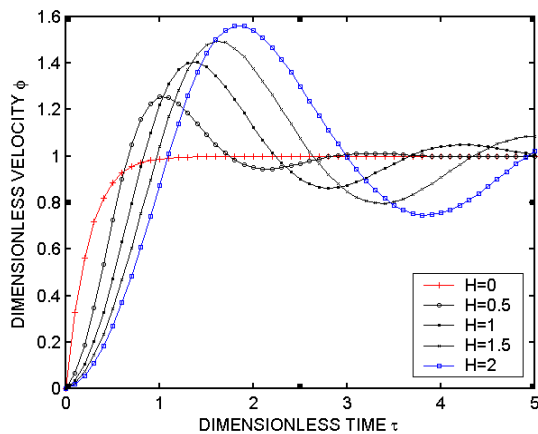


Fig.6 Velocity profiles for a constant pressure gradient under different values of H

For a decreasing exponential input pressure gradient, as shown in Fig. 7, it deserves to pay attention to the fact that the over-shooting effect also appear with a smaller value of H including the Newtonian fluid ($H=0$), which is opposites to that of the increasing input forms.

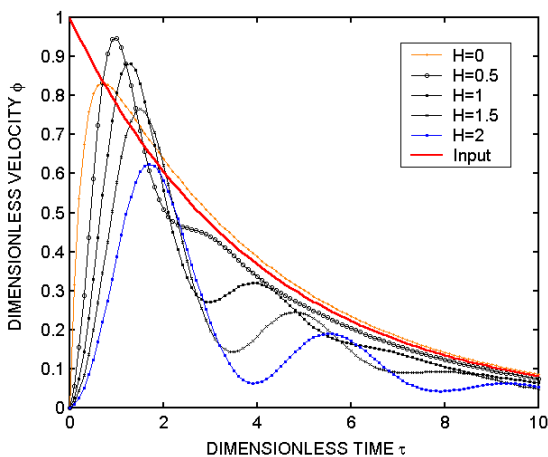


Fig. 7 Central velocity vs. time with varied H

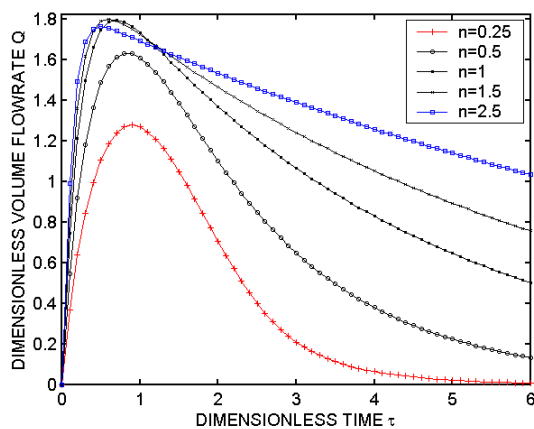


Fig.8 Variations of Q vs. dimensionless time τ with different power-law index n

4.4 Analysis of volumetric flow rate

The analysis of volumetric flow rate is important in dealing with the special, rare and expensive liquids in biochemistry, medicine, medical manufacture and minute chemical engineering. From the analysis of the upper-convected Maxwell fluid model, the volumetric flow rate is fluctuated, and, as the value H increases, the amplitude of over-shooting also increases, as shown in Fig. 8.

5. Conclusions

The characteristics of internal flow fields under different driven pressure function of a micropipette system using the power-law, Carreau and upper-convected Maxwell fluid model are studied. For the power-law fluid, as the index n increases, the time needed to steady state increases. From the analysis of the Carreau model, the velocity of the flow is proportional to the input pressure gradient. If the mass flow rate is fixed, the smaller the radius R of tube, the faster the central velocity. In the study of the upper-convected Maxwell flow, enlarges the value of H increases the amplitude of over-shooting. For volumetric flow rate analysis, the amount of Q increases as the power-law index n decreases in the reinforcing system, while the results is by contraries in decayed pressure system. In conclusion, the results obtained above can serve as the design basis and a reference input of the minute volume control system within the designed control margins

6. References

1. S. Pai, Viscous Flow Theory, 1-laminar Flow. D. Van Nostrand Corp., Princeton N.J., pp. 65-66, 302-303, 1965.
2. RB. Bird, and Stewart, Transport Phenomena. John Wiley and Sons, New York, pp. 126-130, 1966.
3. Brodkey, RS. The Phenomena of Fluid Motion. Addison Wesley, Reading Mass., 1967; 90-95.
4. S. Middleman, Transport Phenomena in the Cardiovascular System. John Wiley and Sons, New York, pp. 29-35, 1972.
5. MN. Lih, Transport Phenomena in Medicine and Biology. John Wiley and Sons, New York, pp. 190-203, 1975.
6. I. Etter, and WR. Schowalter, Unsteady flow of an Oldroyd fluid in a circular tube, Trans. Soc. Rheol., Vol. 9, pp. 351-369, 1965.
7. JK. Okeson, and AH. Emery, Transient development of velocity profiles during shear flow of a viscoelastic fluid, Trans. Soc. Rheol., Vol. 19, pp. 81-98, 1975.
8. H. Schlichting, Boundary Layer Theory, 4th edn., trans. by Kestin, J., McGraw Hill, New York, pp. 72-74, 1960.
9. RK. Bhatnagar, Fluctuating flow of a viscoelastic fluid in a porous channel, J. Appl. Mech., Vol. 46, pp.

21-25, 1979.

10. DP. Ly, and D. Bellet, The study of time-dependent pipe flows of inelastic non-Newtonian fluids using a multiviscous approximation, J. Non-Newtonian Fluid Mech., Vol. 1: pp. 287-304, 1976.
11. RT. Balmer, and MA. Fiorina, Unsteady flow of an inelastic power-law fluid in a circular tube J. Non-Newtonian Fluid Mech., Vol. 7, pp. 189-198, 1980.
12. Giuseppe Pontrelli. Pulsatile blood flow in a pipe Computers & Fluids, Vol. 27(3), pp. 367-380, 1998.
13. RB. Bird, and RC. Armstrong, Dynamics of Polymeric Liquids, Vol. 1, pp. 171-174, 255-263, 1987.
14. KD. Rahaman, and H. Ramkissoon, Unsteady axial viscoelastic pipe flow, J. Non-Newtonian Fluid Mech., Vol. 57, pp. 27-38, 1995.
15. B. Carnahan, and HA. Luther, Applied Numerical Methods, John Wiley and Sons, New York, 1969.
16. Warsi, ZUA. Unsteady flow of power-law fluids through circular pipes, J. Non-Newtonian Fluid Mech., Vol. 55, pp. 197-202, 1994.

圓管內非牛頓流體之驅動流場分析

江新祿¹、馮騰榔¹、洪瑞斌²

¹ 桃園創新技術學院機械工程系

² 國立勤益科技大學機械工程系

摘要

本研究乃針對微滴管系統內部驅動流場進行分析。分析時，從不同的驅動來源，並使用非牛頓流體模型，來得到生化藥劑驅動的不同反應。分析流動時所採用之非牛頓流體模型為冪次律流體、卡瑞爾流體和上層對流麥克斯威爾流體。在研究中考慮了各種變壓力梯度和不同的流體模型。假設圓管內流體流動的初始狀態為靜定，然後一啟動時變壓力梯度施加於圓管內流體。隱式差分法用於獲取流體動量方程式的數值近似解。根據分析結果，不同壓力梯度下，圓管內非牛頓流體之速度分佈，與注入液體積流率和時間之關係可得到。研究之結果，可提供電氣體積流率控制系統設計時，流動參數之參考，使注入液之流量準確地落在控制範圍內。

關鍵字：冪次律流體、卡瑞爾流體、麥克斯威爾流體、微滴管系統